Final Technical Report

Project Title: Lignin as a facilitator, not a barrier, during saccharification by brown rot fungi.

Award Number: GO18088

Recipient: Reagents of the University of Minnesota, Purdue University

Project Location(s): University of Minnesota, Purdue University

Project Period: September 1, 2008 - August 31, 2012
Date of Report: November 28, 2012
Written by: Dr. Jonathan S. Schilling
Program Manager: Dr. Jonathan S. Schilling
Principal Investigators: Dr. Jonathan S. Schilling, Dr. Ulrike Tschirner, Dr. Robert Blanchette, Dr. Timothy Filley

Subcontractors: Dr. Timothy Filley (Purdue University)

Cost-Sharing Partners: Dr. Charles Abbas (Archer Daniel Midland)

DOE Project Team
DOE-HQ contact: Leslie Pezzullo 202-586-1514; leslie.pezzullo@ee.doe.gov
DOE Field Project Officer: Gene Petersen 720-356-1746; gene.petersen@go.doe.gov
DOE Contract Specialist: Geoffrey Walker 720-356-1808; geoffrey.walker@go.doe.gov
DOE Project Engineer: Cynthia Tyler 720-356-1294; cynthia.tyler@go.doe.gov

Acknowledgment: This material is based upon work supported by the Department of Energy under Award Number GO18088.

1. Award Details

Project Title: Lignin as a Facilitator, not a Barrier, during Saccharification by Brown Rot Fungi
Award Number: GO18088
Recipient: Reagents of the University of Minnesota, Purdue University
Project Director: Jonathan S. Schilling (PI)
Co-PIs: Robert Blanchette and Ulrike Tschirner (University of Minnesota), Timothy Filley (Purdue University)
Project Location: University of Minnesota, Purdue University

Date of Report: November 29, 2012
Written by: Jonathan S. Schilling (PI)

Outline **Page**

*2. Protected Data Information (*NA)

3. Executive Summary

This research focused on the biology of a group of wood-degrading fungi that cause brown rot in wood, with particular attention to the potential to mimic this biological approach ex situ for bioprocessing lignocellulosic biomass. During brown rot, fungi remove the sugar component of carbohydrates completely (saccharification) with minimal removal of lignin. This leaves lignin as a by-product of decay and complements the goals of biorefining. In addition, lignin apparently facilitates carbohydrate removal, defying the definition of 'recalcitrance' in biomass. Supported by the long-standing theory that these fungi use a two-step oxidative/enzymatic approach during brown rot, our team's objectives were as follows: **1)** to determine the discrete timing of lignin modifications, **2)** to correlate these alterations with biocatalyst efficiency and ingress into plant cell walls, and **3)** to reproduce modifications prior to saccharification for efficient bioprocessing. The team was organized to efficiently deliver on these goals, and involved cooperators from industry including a cost share partner at Archer Daniel Midland (ADM) Company to consult and guide transition objectives. This project was completed with minimal variance from the original project management plan (PMP), resulting in fourteen presentations and posters, four peer-reviewed publications, and one additional publication now in review. The publications have been valuable to other scientists working toward similar goals and have been cited in thirteen peer-reviewed publications written by others since 2010. We are working with ADM to advance application options for industry, building on the lessons learned during this DOE award period.

The core findings of our research were that 1) lignin modifications occur nearly coincident with enzyme secretion during brown rot and 2) there is no specificity to the benefit that a brown rot pretreatment has on the efficacy of cellulases – it is a general enhancement best predicted by chemical changes to lignin and side-chain hemicellulose sugars. In our work, this meant we could attain and predict broad improvements in saccharification using commercial cellulase cocktails, in some cases more than three-fold of that in untreated biomass. Given its low cost, biological pretreatments using the fungus directly might be competitive, even with slightly lower yields that those attainable on the current biochemical platform. Therefore, one of our publications addressed tissue characters that could be tracked if this were adopted, commercially. In this research, we also attempted to mimick the pretreatment, chemically, and in these cases the kinetics of the reactions resulted in yields lower than those when using the fungus directly. This attempt was complemented by a spatial study to co-localize reaction fronts, where incompatible oxidative and enzymatic reactions co-occurred in discrete space. Combined, these valuable new data sets improve the outlook on an applied mimick and target those mechanisms used by this group of fungi to spatially control reactions to increase yields.

Beyond its applied context, this research provides better understanding of brown rot lignocellulose modifications and a systems perspective (via synthetic biology) on a ubiquitous natural process. This is the first comparative study of tissue modifications during brown rot using three distinct plant sources, conifer, angiosperm, and grass (stover), and results show distinction depending on the feedstock type, particularly in grasses. We have also gone far deeper into a mimick approach than others previously, and our results show interplay and expose potential issues in kinetics in the brown rot paradigm. Combined, the research contributes to information on how these ubiquitous fungi degrade lignocellulosics such as wood, and it benefits science and the public going forward to address carbon cycling, resource conservation, and advanced renewable energy technologies.

4. Proposed vs. Actuals Summary

This section is very brief, given that variances to the project were minor, milestones were reached as planned (given one change to the PMP) and that the deliverables per Task are listed in the following section. The most significant variance was in our approach to microscopic imaging (Task 3), something that demanded a change in the tools used for analysis and pushed the project timeframe back. The goal of this Task did not change, however, and results gave valuable context to results from the other Tasks. In terms of technical barriers addressed, the following is a list of barriers addressed per Task, as outlined in the FY12 PMP.

Task A: Create a time series of brown rot on feedstocks and collect brown rot cellulase preparations. We moved from Technology Readiness Level (TRL) of 1 to 2, and addressed barrier Bt-A, Biomass Fractionation.

Task B: Characterize this decayed material, including their comparative amenabilities to saccharification. We moved from TRL 2 to 3, and addressed barrier Bt-C, Biomass Recalcitrance.

Task C: Use imaging to determine ingress potential of cellulases after brown rot pretreatment of wood. We moved from TRL 1 to 2, although work remains at the TRL level of basic science. In this Task, we addressed barrier Bt-H, Enzyme Biochemistry, as well as Bt-B, Biomass Variability, concerning porosity in the tissue, although this barrier was not listed on our PMP prior to Task.

Task D: Induce plant biomass modifications chemically using elements employed by brown rot fungi. We moved from TRL 3 to 4, and addressed barrier Bt-D, Pretreatment Chemistry.

5. Tasks & Accomplishments

Our proposal had three specific Objectives and a PMP that was organized into four Tasks. Task variances were minor, with the largest change in Task 3 relative to porosity measures using microscopy. The initial grant period was extended from three to four years to accommodate the shift in the imaging approach, and given that change, all milestones and deliverables were accomplished on time. Below are listed the specific Objectives and then the four Tasks with comparison of proposed and actual accomplishments.

5.1. Specific objectives & PMP tasks

Objectives
1. Determine the discrete timing of lignin modifications.
2. Correlate these alterations with the success of enzymatic hydrolysis.
3. Reproduce modifications prior to saccharification for efficient bioprocessing.

PMP Tasks
A. Create a time series of brown rot on feedstocks and collect brown rot cellulase preparations.
B. Characterize this decayed material, including their comparative amenabilities to saccharification.
C. Use imaging to determine ingress potential of cellulases after brown rot pretreatment of wood.
D. Induce plant biomass modifications chemically using elements employed by brown rot fungi.

5.2. Task A

Task A was largely focused on producing, not characterizing, a fungal enzyme stock and a time series of brown rot from early to late decay stages in various relevant feedstocks. Variance from the original proposal was minor, including two additions (one in pre-award) that provided early results leading to two publications (Schilling et al. 2009, Duncan and Schilling 2010). The Deliverables of having both enzymes and decayed substrate in-hand were achieved and the Milestone reached on time and as planned.

5.2.1. Task A logic

To determine how and when plant cell components including lignin are modified during brown rot, we infected woody and non-woody feedstocks with two model brown rot fungi. Plant tissue was harvested and stored after air drying to be characterized using both traditional and cutting-edge analytical methods in Task 2. One of these tissue characters was the amenability of the pretreated biomass to subsequent saccharification, testing for synergy with brown rot cellulases versus stock commercial cellulase preparations. Given that most brown rot fungi lack the key cellulase enzyme type cellobiohydrolase (CBH), we expected we might see a benefit of brown rot tissue modifications on their own enzyme system using a crude extract approach, versus any benefit using commercial cellulases from *Trichoderma* spp. and other fungi. This is a pattern seen in nature known as 'home field advantage,' where biomass degraded by a particular fungus and then sterilized and exposed to a consortium of potential colonizer fungi will inevitably be re-colonized by the same original decay species. Any synergy between pretreatment and saccharification would be clearly worth pursuing in application on the biochemical platform, yet this had not been tested.

5.2.2. Obtaining feedstocks

Tasks A.1 and A.2 were to acquire and then colonize three lignocellulose feedstocks, respectively, using several different model brown rot fungi. The Milestone for Task A was to have harvested biomass over a decay time series up to 4 months, along with the enzyme extracts from solid-state culturing required to move on to Task B. The approaches and fungi used in Task A are very familiar to the research team, but they take a long time relative to typical microbial trials. This Task was easily accomplished within the allotted time period.

Aspen, spruce and corn stover were selected as viable bioenergy feedstocks that also represent a range of plant types, useful for making comparisons. Aspen (*Populus* sp.) and spruce (*Picea* sp.) 19-mm cubes were cut from single, non-treated boards acquired from a local lumber supplier in Minneapolis, Minnesota, USA. Corn (*Zea mays*) stover was acquired from a farm co-operative in Pine City, Minnesota, and stems and leaves were homogenized in a Wiley mill to pass through a 40 mesh screen. Wood was oven-dried at 100°C for 48 h to determine initial weight. Stover powder was partitioned into 1 g aliquots and oven-dried for addition to soil-block microcosms. All substrates were then autoclaved at 121°C for 1 h to sterilize.

5.2.3. Fungal degradation of feedstock substrates

Wood blocks were degraded using the ASTM soil-block jar method (ASTM 2007, D 1413-07) for 1, 2, 4, 8, or 16 weeks using one of two test brown rot fungi, *Gloeophyllum trabeum* (Fr.) Murr. (isolate ATCC 11539) or *Postia placenta* (Fr.) M.J. Larsen & Lombard (isolate MAD 698). Five

blocks were added per jar for a time series, and single-block harvests were made aseptically. Corn stover was degraded in modified soil-block jars. The 1 g aliquot of stover was added to a 15 ml PTFE centrifuge tube cut in cross section so that the lip of the tube, thrust into the soil between two inoculated birch feeder strips, was flush with the soil surface. This allowed fungal inoculum to grow over the lip of the tubes and down into the stover, with one tube per soil-block jar. Incubation was at room temperature in the dark. All fungus-feedstock treatments were replicated five times (n=5), totaling 50 stover jars and 20 wood cube jars. Included also were 15 non-inoculated jars with fungus-free agar and a replicate set for each feedstock to serve as time zero, non-decayed control material.

Wood blocks were harvested and weighed fresh and a small portion was oven-dried to determine weight loss. The large portion was air-dried at 30°C for 7 d, Wiley milled to 40 mesh, and stored over desiccant prior to saccharification. In the case of stover powders, characterization of carbohydrate and lignin fractions was used instead of weight loss to infer decay progress, and powders were air-dried and stored over desiccant, similar to wood samples.

We also had initiated a similar trial prior to the award period during pre-award status because we were keen to accelerate our progress toward resolving the question of synergy within the brown rot mechanism. That trial utilized spruce and southern yellow pine blocks of the same dimensions and decayed by the brown rot fungi *Gloeophyllum trabeum* (Fr.) Murr. (isolate ATCC 11539) or *Fomitopsis pinicola* (Swartz:Fr.) Karst. (isolate FP 105877R). The *F. pinicola* was not sequenced or annotated at the time, but provided a contrast that was relevant when utilizing two conifers, pine and spruce. That trial was completed after this grant cycle had begun, at week 8, and we took that opportunity to include a third variable of pretreatment with dilute acid (DA). This provided a commonly used standard for comparison to brown rot modifications, and gave perspective on the relative efficacy as well as tissue modification comparisons against something more commercially well-known. Non-degraded spruce and pine powders (40 mesh) were treated separately with 0.5% (v/v) H_2SO_4 at 170°C for 2 h using constant rotation and a feedstock/acid ratio of 1:6 (w/v). Acid-hydrolyzed feedstock was filtered, rinsed with water, air-dried, and stored over desiccant. This material, and its analysis, was the basis for our first paper (Schilling et al. 2009), while the experimental design describe at the beginning of this section was a different paper (Schilling et al. 2012) that included analyses of tissue modifications as correlative values.

5.2.4. Enzyme extract collection

Celluclast 1.5L (Sigma, St. Louis, MO, USA) and Novozyme 188 (Sigma) were used to saccharify degraded wood or stover. Combined with the fact that hemicellulase activity remains in fungal crude extracts as well as in Celluclast 1.5L, hemicellulose saccharification yields were included in the results. Cellulase extracts from the two test fungi were used to saccharify substrates in order to compare gains in saccharification efficiency provided by brown rot pretreatments and to ensure that pretreatment effects were robust and not specific only to brown rot enzymes. Fungal extracts were acquired from solid-state cultures and concentrated/desalted, using 212 g of aspen, spruce, pine, or stover powder, along with 12 g wheat bran, 25 g millet, and 250 mL water, to provide the enzyme extracts to be used to test 'home field advantage' for brown rot enzymes.

Extract was passed through a PD-10 desalting column, concentrating the extract 16-fold (v/v). Both solid and liquid concentrated extracts were collected over ice and stored at −70°C prior to use. Liquid state and solid state cellulase extracts were evaluated for protein concentrations

(mg/mL) before and after concentration/desalting protocols. Protein concentrations were measured with Coomassie® Brilliant Blue G-250 dye (Bio-Rad). Increases in protein concentrations were compared to the extracts' preliminary concentrations to determine the amount of proteins lost during extraction procedures. Endo-β-glucanase levels were measured by testing action on azo-dyed carboxymethylcellulose (Megazyme, Bray, Ireland) and were quantified as carboxymethyl cellulose units (CMCU). The β-glucosidase activity was tested by measuring action on p-nitrophenol-β-D-glucopyranoside and quantified as p-nitrophenol-β-D glucopyranoside units (pNPGU). Total cellulase activity levels were evaluated by testing action on crystalline filter paper (Whatman #1) and quantified as standard filter paper units following the DOE-NREL standard. When used to standardize loading potentials, all enzyme activities including CMCU, pNPGU, and FPU are displayed relative to one gram of cellulose.

Because it took several tries to optimize the solid-state conditions for growing the fungus and extracting high titers of enzyme, we expanded the feedstock substrates included, once optimized, from four to six by including mixed prairie grasses and a dicot, alfalfa. We also used *Trametes versiscolor* as a positive control. This, along with a broader range of enzyme activity assays using the same colorimetric approach, allowed us to use the solid-state system meant to generate enzyme stock for Task 2 to act as a stand-alone trial at very low cost. This generated very interesting results showing that the constitutive cellulase production of a brown rot is not matched by equal hemicellulase production. Instead, it depends on both the chemistry and the morphology of the feedstock, and this was published as Duncan and Schilling (2010).

5.3. Task B

Task B was focused on characterizing the time series of decayed lignocellulosic substrates, including their amenability to cellulases. The Deliverables were material characterization and saccharification yield comparisons between native brown rot cellulase extracts and commercial cellulase. Both were achieved with little variance from the proposed Task, and the Milestone was reached on time. Results from this effort led to two publications (Schilling et al. 2009, Schilling et al. 2012).

5.3.1. Task B logic

This effort was geared toward characterizing 1) the physiochemical attributes of three distinct feedstock types (spruce, aspen, stover) decayed in a time series, 2) the amenability of these substrates decayed to various degrees to being enzymatically hydrolyzed, and 3) the correlation between these tissue modifications and their hydrolytic amenability. As stated for Task A, the assumption was that there might be 'home field advantage' for brown rot enzyme suites on brown rotted substrates, in which case a synergy might be possible between commercial pretreatments and saccharification steps. Particular focus was on lignin modifications because of the apparent facilitation of brown rot in the presence of lignin. This defies the definition of 'recalcitrance' in biomass – lignin is typically viewed as the key barrier to biomass conversion on the biochemical platform.

5.3.2. Weight loss and wet chemistry

As mentioned in section 4.2.3., wood and stover were harvested and a small portion used to determine moisture content. Fresh whole-block weights were then adjusted using a moisture

correction factor and the block weight losses were calculated (Table 1). Stover weight loss was not possible in our design, and wet chemistry was used to infer decay progress (Table 2). One of our test fungi, *P. placenta*, could not apparently degrade stover in this experimental design, and we did follow-up using whole stalk corn stover in a standard ASTM soil-block design. Even in this set-up, however, *P. placenta* did not degrade stover, and we have now observed this multiple times without exception. We first reported this in Duncan and Schilling (2010) but showed this pattern more explicitly in Schilling et al. (2012). It is an interesting finding, given the high p-coumaryl content in the lignin of grasses like corn stover. In a separate research project, we have further pursued this phenomenon by testing *Fomitopsis pinicola* as well as many other *Postia* spp., with results that elucidate evolutionary connections and the role of lignin.

For all samples, lignin, cellulose, hemicelluloses, and solubilized glucan and xylan were determined (Tables 1 and 2). This was done gravimetrically or via high performance liquid chromatography (HPLC) as oven-dry weight percents. Powder obtained from grinding the small block portions, plus DA samples, were analyzed following the TAPPI standard protocol for acid-insoluble lignin (TAPPI T 222 om-23). Carbohydrate content was determined by analyzing the filtrate after acid-insoluble lignin removal. The filtrate was passed through a GHP 0.2 μm filter and was analyzed using HPLC. Glucose, xylose, galactose, arabinose, and mannose were separated, along with a cellobiose internal standard, using a de-ashing guard column (Bio-Rad, Hercules, CA, USA) and a 300 x 7.8 mm Metacarb 87P analytical column (Varian, Les Ulis, France). Column temperature was 80°C, mobile phase was deionized water at a flow rate of 0.3 ml min^{-1}, and detections were made using refractive index. Acid-insoluble lignin was ashed at 575°C for stover in order to subtract inorganics (specifically silica) from the acid-insoluble lignin fraction. Solublized glucan and xylan fractions were measured in enzyme-free saccharification blanks. This fraction was included in calculations of glucan-to-glucose saccharification yields (useful for determining overall percent-of-original yields) or subtracted during calculations of cellulose-to-glucose yields (useful for determining specifically the effect of pretreatment in enhancing enzyme hydrolysis).

5.3.3. Tissue characterization

For the work leading to the Schilling et al. (2012) publication, cellulose crystallinity was measured using X-ray diffraction (XRD) in five replicates from time zero material and for each replicate sample harvested at weeks 8 and 16 (Table 3). This use of XRD instead of solid-state (ss) NMR, as proposed, was a variance that became most logical given the results obtained from NMR. Using magic angle spinning with the ssNMR resulted in poor peak resolution and difficulty obtaining precision among technical replicates. This was due to integration issues, and in short, we determined that having XRD and the thermochemolysis technique at Purdue University made using ssNMR redundant, if not unreliable. Corn stover was heavily degraded by *G. trabeum* and there was not enough material for XRD in weeks 8 and 16. Measurements were made using standard volumes of air-dried 40-mesh powders. Crystallinity was measured using a Bruker-AXS D5005 (Siemens AG, Erlangen, Germany) XRD and at a voltage of 45 kV and current of 40 mV. The samples were scanned over a range from $2\theta = 5^{\circ} - 40^{\circ}$ at a scan rate of $0.048^{\circ}/s$. Following Segal et al. (1959) setting I_{002} as the intensity of the crystalline peak at about $2\theta = 22.5°$ and I_{am} as the intensity at $2\theta = 18.7°$, crystallinity was calculated as an index (CrI) using peak area comparisons, an approach verified by other groups and cited in the Schilling et al. (2012) paper.

Lignin demethylation and side chain oxidation were measured over the time series using ^{13}C-tetramethylammonium (^{13}C-TMAH) thermochemolysis (Table 3). Single culture decomposition

Table 1 – Wood % weight loss (standard error, n=5), and carbon fractions in aspen or spruce blocks decayed as a pretreatment over a 16-week time series by either *Gloeophyllum trabeum* or *Postia placenta*, two brown rot fungi.

Fungus / Wood	Week	% Weight Loss	Adjusted[a] Wt.% Lignin	Glucan	Xylan	Galactan	Arabinan	Mannan	Sum Hemi-cellulose
	0	-	27.1	42.1	8.4	1.4	2.8	3.7	16.2
	1	1.0 (2.7)	27.6	43.2	10.6	0.7	0.8	1.8	14.0
G. trabeum	2	18.8 (2.1)	22.3	29.5	7.3	1.0	1.2	0.9	10.5
/ Aspen	4	28.6 (2.7)	24.7	24.6	5.1	0.5	0.4	0.5	6.5
	8	38.1 (2.1)	24.9	18.8	3.4	0.5	1.0	0.6	5.4
	16	57.9 (3.4)	20.9	9.1	1.9	0.6	0.2	0.2	2.9
	0	-	27.1	42.1	8.4	1.4	2.8	3.7	16.2
	1	0.2 (0.6)	28.6	38.4	8.6	0.7	1.9	1.8	13.0
P. placenta	2	1.7 (0.9)	21.8	40.6	10.2	0.7	2.1	2.1	15.1
/ Aspen	4	0.8 (1.5)	19.4	41.0	10.4	0.7	2.4	2.6	16.0
	8	17.9 (3.3)	18.5	30.3	8.3	0.7	2.0	2.0	13.0
	16	34.2 (4.5)	15.0	22.2	5.4	0.5	0.9	1.0	7.7
	0	-	31.7	36.0	5.8	5.7	5.0	9.4	25.8
	1	3.8 (4.1)	30.7	39.2	3.2	0.8	1.4	9.0	14.5
G. trabeum	2	10.7 (5.6)	33.5	32.7	3.5	1.6	1.1	6.6	12.8
/ Spruce	4	19.5 (4.2)	30.8	29.2	2.6	0.5	0.4	5.2	8.7
	8	35.9 (2.9)	26.3	21.7	1.7	0.4	0.9	3.9	6.9
	16	53.6 (2.2)	21.4	12.2	1.1	0.7	0.6	2.6	5.0
	0	-	31.7	36.0	5.8	5.7	5.0	9.4	25.8
	1	0.0 (2.2)	27.5	43.4	5.7	1.4	1.4	12.0	20.6
P. placenta	2	0.2 (1.4)	30.5	42.6	4.3	1.1	1.3	10.7	17.3
/ Spruce	4	7.0 (2.4)	30.6	36.8	3.8	1.3	1.1	8.8	15.0
	8	15.7 (2.7)	29.9	33.0	3.2	0.8	0.8	6.7	11.6
	16	36.5 (4.8)	29.8	18.2	1.9	0.7	0.42	3.6	6.6

[a] Duplicate characterizations from homogenized powder - equal parts of five separately-decayed replicates. Data adjusted to compensate mass loss by multiplying by the average fraction of weight remaining in blocks (oven-dry).

Table 2 – Non-adjusted[a] lignin, glucan and hemicellulose fractions, plus saccharification yields in corn stover decayed over a 16-week time series by a brown rot fungus, either *Gloeophyllum trabeum* or *Postia placenta*.

		Constituent (Non-adjusted[a] Wt.%)								
Fungus	Week	Lignin	Glucan	Xylan	Galactan	Arabinan	Mannan	Sum Hemi-cellulose	*Native*[b] Cellulose-to-glucose	*Cell/Novo* Cellulose-to-glucose
	0	25.9	32.6	8.3	1.0	4.0	0.4	13.7	7.1 (0.2)	29.2 (1.2)
	1	24.5	30.8	7.2	0.8	3.3	0.4	11.7	3.9 (0.1)	30.8 (0.2)
G.	2	24.4	30.5	7.5	0.8	3.7	0.4	12.4	12.7 (2.4)	31.4 (0.4)
trabeum	4	26.8	28.6	6.9	0.5	3.2	0.4	11.0	16.5 (0.1)	38.7 (0.8)
	8	33.2	22.3	5.1	0.7	1.7	0.4	7.9	15.4 (0.2)	44.0 (0.0)
	16	39.6	14.0	3.0	0.3	2.1	0.7	6.1	11.5 (0.1)	21.9 (0.0)
	0	25.9	32.6	8.3	1.0	4.0	0.4	13.7	6.1 (0.6)	12.8 (0.6)
	1	26.5	32.7	8.5	0.9	3.3	0.7	13.4	3.2 (0.4)	27.1 (1.6)
P.	2	25.5	33.3	7.9	0.7	3.2	0.4	12.2	4.1 (0.1)	25.7 (0.4)
placenta	4	24.3	33.0	8.5	0.8	3.2	0.4	12.9	3.2 (0.6)	24.0 (0.6)
	8	26.4	33.6	7.9	0.5	3.5	0.5	12.4	1.7 (0.3)	23.8 (0.8)
	16	24.7	32.6	8.3	0.7	3.1	0.4	12.5	1.8 (0.3)	25.0 (0.1)

[a] Duplicates run on homogenized milled powder from five separately-degraded replicates. Weight% data could not be adjusted to reflect density loss because it was decayed as a loose powder. The trend of each constituent is therefore relative to other constituents. [b]"Native" is brown rot extracts, and "Cell/Novo" is Celluclast and Novozyme, not at full FPU.

Table 3 – Cellulose crystallinity index (CrI), lignin side chain oxidation (G6/G4; S6/S4), and selected lignin demethylation (standard deviations) in wood decayed by *G. trabeum* or *P. placenta*, measured by XRD or ^{13}C-TMAH thermochemolysis. CrI replication was n=5, while TMAH data is from duplicate analyses of homogenized wood powder.

Fungus / Wood	Week	CrI (%)	S/G[a]	G6/G4[b]	S6/S4[c]	%dm G14+15[d]	%dm S15[e]	%dm G4[f]	%dm G6[g]
G. trabeum / Aspen	0	56.4 (3.9)	1.6 (0.1)	0.3 (0.0)	0.3 (0.0)	1.1 (0.2)	2.7 (0.5)	5.5 (0.6)	18.7 (1.5)
	2	-	1.8 (0.6)	0.4 (0.2)	0.7 (0.4)	4.1 (0.8)	10.0 (1.7)	14.7 (1.5)	46.1 (1.7)
	4	-	1.6 (0.4)	0.6 (0.3)	0.6 (0.2)	4.6 (0.8)	10.2 (1.4)	14.0 (1.6)	37.7 (0.8)
	8	48.0 (3.2)	2.2 (0.6)	1.1 (0.2)	1.1 (0.4)	4.7 (0.8)	8.9 (1.7)	14.4 (1.5)	47.5 (1.7)
	16	40.5 (4.4)	1.9 (0.4)	1.5 (0.3)	1.1 (0.2)	5.7(0.8)	14.4 (4.6)	15.6 (1.6)	52.1 (0.8)
P. placenta / Aspen	0	56.4 (3.9)	1.6 (0.1)	0.3 (0.0)	0.3 (0.0)	1.1 (0.2)	2.7 (0.5)	5.5 (0.6)	18.7 (1.5)
	2	-	1.6 (0.2)	0.3 (0.1)	0.4 (0.1)	1.5 (1.1)	0.9 (1.7)	7.2 (1.5)	20.9 (0.4)
	4	-	1.4 (0.4)	0.6 (0.4)	0.5 (0.2)	3.8 (0.8)	3.9 (2.0)	9.8 (1.5)	23.8 (0.8)
	8	52.3 (1.9)	1.8 (0.2)	1.4 (0.2)	0.8 (0.1)	2.9 (1.0)	6.7 (1.2)	12.0 (1.6)	41.4 (0.5)
	16	50.4 (3.4)	1.9 (0.3)	1.2 (0.3)	0.9 (0.1)	2.5 (1.6)	6.7 (0.8)	12.6 (0.6)	42.9 (1.3)
G. trabeum / Spruce	0	48.5 (0.7)	-	0.3 (0.0)	-	1.1 (0.3)	-	4.5 (0.5)	11.4 (3.6)
	1	-	-	0.5 (0.2)	-	1.3 (0.2)	-	6.3 (1.6)	10.9 (3.5)
	2	-	-	0.7 (0.1)	-	2.1 (0.5)	-	8.4 (1.6)	14.9 (1.3)
	4	-	-	0.7 (0.3)	-	4.1 (0.6)	-	10.7 (1.8)	18.2 (1.8)
	8	45.4 (3.9)	-	0.8 (0.1)	-	5.7 (0.9)	-	11.5 (1.3)	17.2 (0.6)
	16	38.2 (4.4)	-	0.8 (0.1)	-	8.0 (3.7)	-	15.4 (3.7)	21.4 (1.0)
P. placenta / Spruce	0	48.5 (0.7)	-	0.3 (0.0)	-	1.1 (0.3)	-	4.5 (0.5)	11.4 (3.6)
	1	-	-	0.5 (0.2)	-	1.2 (0.2)	-	4.3 (1.6)	10.9 (3.5)
	2	-	-	0.7 (0.1)	-	2.1 (0.5)	-	8.2 (1.6)	14.8 (1.3)
	4	-	-	0.6 (0.2)	-	3.0 (1.2)	-	6.8 (1.9)	14.1 (2.8)
	8	51.1 (3.2)	-	0.7 (0.3)	-	5.3 (1.0)	-	11.8 (1.5)	17.7 (1.1)
	16	40.8 (4.2)	-	0.7 (0.1)	-	5.7 (1.6)	-	13.4 (0.9)	19.0 (1.0)

[a] Syringyl/Guaicyl (S/G) ratio; [b,c] Ac/Al in G and S (spruce has no syringyl units); [d] %demethylation of averaged G14 and G15; [e] %demethylation of S15 in the angiosperm, aspen; [f,g] %demethylation of G4 and G6. Note: week 1 aspen samples were not available in enough volume for analyses.

experiments within our group (Filley, Purdue University) have demonstrated that during both brown and white rot decay the relative proportion of permethylated vanillic acid (G6) to vanillin (G4) (G6/G4), or also commonly termed acid to aldehyde- Ac/Al, increases progressively. This increase is thought to be indicative of oxidative alteration of the alpha carbon on the propanoid chain in lignin which decomposes to vanillic acid during TMAH thermochemolysis. ^{13}C-TMAH thermochemolysis and analysis was performed in-line with a Pyr-4a pyrolysis unit (Shimadzu Scientific Instruments, Columbia, MD, USA) interfaced to a GC17A gas chromatograph with peak detection by a QP5050A quadrupole mass spectrometer (Shimadzu). Samples were weighed (≈150 μg) into 3 mm platinum buckets containing 200 ng of an eicosane internal standard. Next, 3 μl of a 50 wt% solution of ^{13}C-TMAH in degassed, dionized water was added. The bucket was placed in the Pyr-4a at room temperature for 5 min under a He gas stream, then heated to 350°C. The injector base of the Pyr-4a was maintained at 320°C and with a split flow of 20/1. Chromatographic separation was performed on an RTx-5 (Restek Corporation, Bellefonte, PA, USA) fused silica column (30 m, 0.25 mm i.d., film thickness 0.25 μm). The oven was ramped from 60°C (1 min stationary) to 300°C at 7°C min^{-1} with a hold time of 15 min. Mass spectra were collected over a range from 40–550 amu.

Chromatograms were analyzed for methylated syringyl (S), guaiacyl (G), and p-coumaryl (P) phenols in order to determine the extent their relative yields, lignin side chain oxidation, and extent of fungal demethylation (Filley et al. 2003). The methylated phenols released in the TMAH chemolysis were analyzed for their original aromatic methoxyl/hydroxyl content by determining the number of ^{13}C-labeled methyl groups added during the procedure using mass spectrometry. Analysis permits, for example, resolution of whether observed 3,4-dimethoxy structures are of native guaiacyl (as 3-methoxy, 4-hydroxy substitution), or orthodihydroxy (3,4-dihydroxy substitution) that are produced due to progressive brown rot demethylation of lignin.

5.3.4. Enzymes and saccharification

Both brown rot fungal extracts from solid-state culturing as well as commercially available Celluclast 1.5L (Sigma, St. Louis, MO, USA) and Novozyme 188 (Sigma) were used to saccharify degraded wood or stover. Because hemicellulase activity remains in fungal crude extracts and Celluclast has hemicellulase activity, hemicellulose saccharification yields are included in the results. Cellulase extracts from the two test fungi were used to saccharify substrates in order to compare gains in saccharification efficiency provided by brown rot pretreatments and to ensure that pretreatment effects were robust and not specific only to brown rot enzymes. Fungal extracts were acquired from solid-state cultures and concentrated/desalted following Tewalt and Schilling (2010), with aspen, spruce, or stover powder substituting for the 212 g of pine used previously. Protein concentrations, measured using Protein Assay Kit I (Bio-Rad, Hercules, CA, USA), were used to determine efficacy of concentrating and desalting steps.

Because these brown rot extracts have little or no activity on crystalline cellulose when using the standard filter paper units (FPU) assay, commercial and crude extracts were loaded at equal endoglucanase activity. Endo-β-glucanase activity was measured on azo-dyed carboxymethylcellulose (CMC) (Megazyme, Bray, Ireland) and quantified as CMC units, or CMCU. β-glucosidase activity was measured as p-nitrophenyl-β-D-glucopyranoside units (pNPGU), as outlined in the Tewalt and Schilling (2010) paper. Commercial cellulase activity was evaluated using an additional assay with Whatman #1 filter paper (Whatman, Kent, UK) and expressed as FPU. Standard loading potentials are, in each case, relative to one gram of cellulose.

The endoglucanase-limited loadings for *Gloeophyllum trabeum* and *Postia placenta* extracts were 1880 CMCU and 720 CMCU, respectively. In order to test synergy specifically between pretreatment and brown rot enzymes, commercial enzymes were added at these low endoglucanase titers, which are respectively 50% and 19% of the CMCU in the NREL LAP full charge of 60 FPU. Novozyme 188, the β-glucosidase, was added at 41.2 pNPGU and 15.6 pNPGU, respectively, to remove limitation of cellobiose hydrolysis. To assess yields at full strength enzyme loading, the two best-yield samples were selected for each test fungus for saccharification at 60 FPU (in this case 3727 CMCU) and at 64 pNPGU. Saccharification conditions were with rotation (68 rpm) at 50°C, for 12 days ensuring completion.

Hydrolysates from saccharified feedstocks were analyzed via HPLC following a similar protocol to that described in section 4.3.2 but without a de-ashing column for acidic samples. Hydration conversion factors were applied to hydrolyzed carbohydrates. Soluble glucan fractions were measured from the enzyme-free blanks, and used toward calculating sugar yields as absolute cellulose-to-glucose conversion after pretreatment as well as the yields of sugars relative to the initial contents in the feedstocks. The Schilling et al. (2009) paper has a detailed description of yield calculations, which are not trivial and are depicted below in Figure 1. In order to monitor actual conversion efficiency (cellulose hydrolyzed to glucose) instead of total sugar yield, Equation 1 was used to subtract free glucose present in the samples prior to hydrolysis. Equation 2 gives total glucose present after saccharification, regardless of extent of substrate decay. Equation 3 compensates for glucose consumed by the fungi, with yields based on original glucan content.

(1) Actual saccharification cellulose-to-glucose (%): (A3-A2/B2-A2)*100

(2) Total saccharification glucan-to-glucose (%): (A3/B2)*100

(3) Mass loss-compensated glucan-to-glucose (%): (A3/B2)*(1-(X/100))*100

A glucan content of 40% in a wood having lost 25% of its original mass is not the same as 40% in non-decayed wood. If the goal is to quantify yield based on contents prior to pretreatment, 40% must be multiplied by a mass loss conversion factor of 0.75 yielding 30% as 'normalized' content.

5.3.5. Targeted time series

In the work leading to the Schilling et al. (2012) paper, glucose yields after saccharification were most promising for *G. trabeum* degraded aspen. Given this promising yield using the fungus as a direct pretreatment, we designed a second decay series using ASTM microcosms, as before, but including a more resolved time series with many more harvests within this 'target zone' of yields. Harvests were made around the time point of highest yields in the first experimental time series (day 14), with harvests made every two days starting on day 8 and ending on day 34. Residues were harvested and handled in the same manner as before, but only characterizing weight-based lignin, cellulose, and xylan fractions and saccharifying using full strength Celluclast 1.5L and Novozyme 188. The goal was to overlay the timing of yields with the tissue characteristics that might help someone predict them (Figure 2).

Saccharification yields were tracked with more resolution in our follow-up trial with *G. trabeum* on aspen. Yields are expressed both relative to the original glucan content and relative to glucan

Table 4 – Cellulose-to-glucose[a] (wt%) (std dev) (Cell-to-gluc) and hemicellulose-to-monomer (Hem-to-monomer) yields (equal CMCU[b]) of feedstocks decayed up to 16 wks by *Gloeophyllum trabeum* or *Postia placenta*.

Enzyme Source	Week	Fungus/feedstock (Cell-to-gluc)				Fungus/feedstock (Hem-to-monomer)			
		Gt[c] aspen	*Gt* spruce	*Pp* aspen	*Pp* spruce	*Gt* aspen	*Gt* spruce	*Pp* aspen	*Pp* spruce
Native[d]	0	4.3 ± 0.5	3.3 ± 0.3	2.9 ± 0.6	0.7 ± 0.0	15.2 ± 0.4	5.2 ± 0.2	6.5 ± 1.6	1.6 ± 0.3
	1	3.3 ± 0.3	3.9 ± 1.1	1.6 ± 0.2	1.3 ± 0.0	11.2 ± 0.4	13.4 ± 0.6	3.3 ± 0.4	9.5 ± 0.3
	2	8.1 ± 0.9	7.1 ± 0.3	1.6 ± 0.3	1.2 ± 0.0	20.9 ± 0.3	17.1 ± 1.0	8.2 ± 0.6	10.3 ± 0.2
	4	7.9 ± 1.1	4.0 ± 1.5	1.5 ± 0.3	0.9 ± 0.2	21.7 ± 2.0	32.6 ± 2.2	6.7 ± 0.5	11.2 ± 0.8
	8	8.0 ± 1.5	4.1 ± 0.7	3.2 ± 0.9	2.2 ± 0.3	25.1 ± 1.2	18.7 ± 1.0	10.0 ± 1.1	18.3 ± 0.4
	16	7.8 ± 1.6	3.8 ± 0.9	1.6 ± 0.2	2.8 ± 0.4	15.7 ± 2.5	19.7 ± 0.1	14.8 ± 0.4	9.8 ± 0.3
Celluclast + Novozyme	0	24.7 ± 0.9	13.3 ± 0.4	8.6 ± 0.2	6.3 ± 0.2	17.3 ± 0.6	5.0 ± 0.6	12.0 ± 0.1	4.6 ± 0.1
	1	26.8 ± 0.3	12.7 ± 0.6	10.3 ± 0.6	9.6 ± 0.3	18.4 ± 0.8	12.6 ± 0.5	11.6 ± 0.6	8.2 ± 0.0
	2	**47.8 ± 1.3**[e]	11.6 ± 0.1	10.7 ± 0.1	8.9 ± 0.2	**39.1 ± 1.4**	13.6 ± 0.3	11.6 ± 0.5	7.6 ± 0.2
	4	42.9 ± 0.3	15.1 ± 0.3	14.1 ± 0.1	11.7 ± 0.7	31.5 ± 1.1	20.4 ± 0.9	11.0 ± 0.2	6.3± 0.3
	8	41.8 ± 1.3	19.2 ± 0.8	**29.3 ± 0.5**	19.3 ± 1.3	39.0 ± 1.5	14.9 ± 0.1	**16.4 ± 0.4**	14.7 ± 0.7
	16	36.2 ± 1.5	12.1 ± 0.5	18.1± 0.2	14.3 ± 0.8	26.7 ± 0.2	6.0 ± 0.4	20.8± 0.0	13.5 ± 0.7

[a]Calculated by subtracting soluble glucan measured in enzyme-free blanks. [b]Loaded at equal CMCU, within a fungal species, forcing the Celluclast FPU to 65% and 24% of a full strength in *G. trabeum* and *P. placenta*, respectively. [c]*Gt* = *G. trabeum*, *Pp* = *P. placenta*. [d]'Native' is crude extract from solid-state cultures of the same fungus used to pre-treat material. [e]Means in **bold** selected to re-saccharify at full FPU strength.

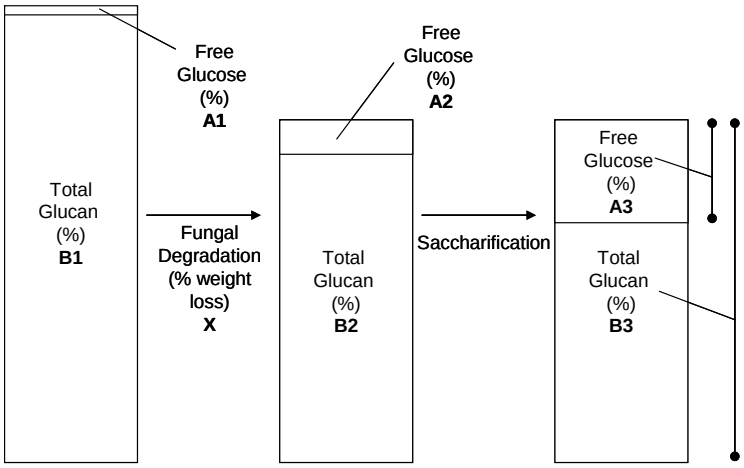

Figure 1 - Glucan (polysaccharides + glucose) fraction inventory for calculating relevant yields of 1) glucose derived from cellulose, not including 'free' glucose, 2) glucose as a fraction of glucan available after fungal pretreatment and loss of mass, and 3) glucose per original glucan in untreated biomass, compensating for glucose consumed by the fungus. B1, B2, A2, and A3 measured directly with mass loss (X).

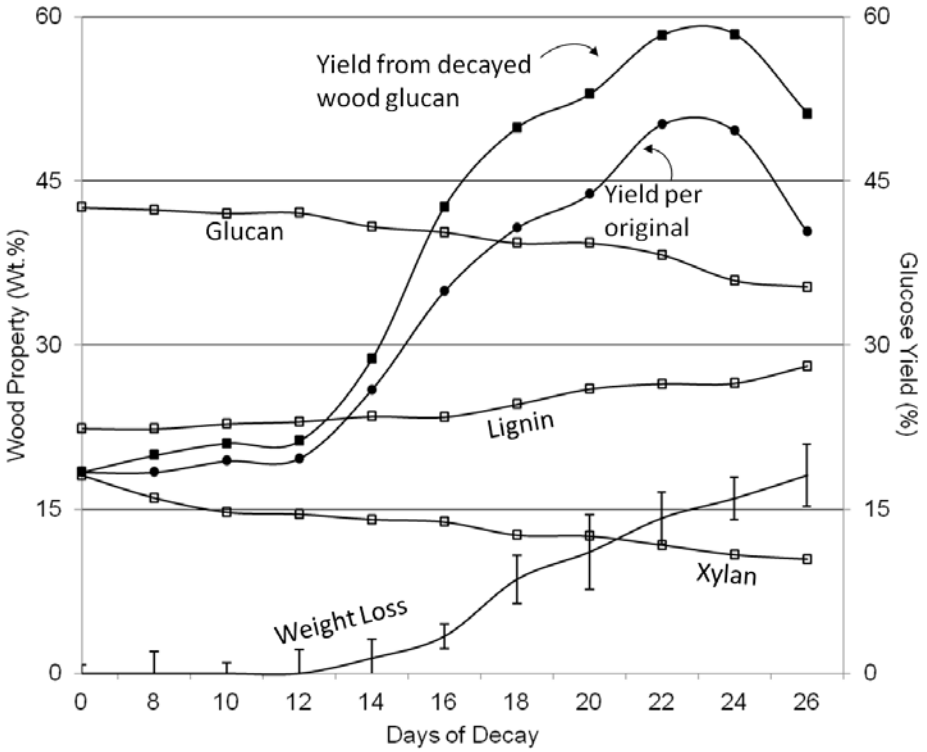

Figure 2 - Yields of glucose after saccharification of aspen pre-degraded by *G. trabeum* to various extents. Yields relative to initial diverge due to progressive metabolism of glucan by the fungus during decay. Weight percent carbon fractions are plotted along the same time series. The wt% was not adjusted for mass loss in order to show characters as they would be measured in a batch process using fractionated biomass.

remaining after fungal pretreatment and metabolism (Figure 2). Yields peaked at day 24 relative to post-decay glucan (58.4%) and at day 22 relative to original glucan (50.2%). By targeting this more thorough time series, we increased resolution to better predict when you would achieve the highestyield, showing divergence relative to initial and post-decay glucan after a short incubation period. The later timing of the optimum harvest point in the follow-up trial also highlights run-to-run variability that can occur when using a fungus. This variability supports the idea that finding reliable, predictive tissue characters is useful for inferring pretreatment severity in future batch processing of material.

5.3.6. Conclusions from Task B

This Task provided insight into the decay mechanism, as well as the potential for brown rot as a pretreatment of lignocellulose. Concerning the first insight, it was evident from the work in the Schilling et al. (2009) paper as well as the Schilling et al. (2012) paper that no synergy between brown rot pretreatments and enzymes was apparent. This is striking, given the simple cellulase system of brown rot fungi. By using crude extracts as we did, we should have been able to detect interplay between early tissue modifications and enzyme efficacy, but commercial enzymes performed better and had similar increased efficacy after brown rot pretreatment. This broad improvement in enzyme efficacy meant that we could attain >50% yields of glucose per original glucan content using commercial cellulase mixtures, a noteworthy yield given the ease of pretreatment. This kind of biological pretreatment was not our intent, but our detailed characterization allowed us to follow up in a second way by detailing the correlation between tissue modifications and yields. Lignin demethylation best fit the timing of yield increases, an interesting interplay that may relate to its active role in brown rot. Overall, this Task was a success and yielded excellent results in both fundamental and applied contexts.

5.4. Task C

This Task was focused on spatially localizing the two key steps in brown rot, the oxidative Fenton-based pretreatment and the cellulolytic saccharification step with enzymes. The original proposal was to track ingress of the brown rot endoglucanase using gold-labeled antibodies and electron microscopy, and it was adapted during the award period to obtain the same spatial information but with a slightly different set of tools. This Task also required hire of someone capable on the microscopy front, for which we experienced some delay. This, along with the change in tack, was the basis for a no-cost extension one additional year. The Deliverables for testing ingress were met shortly after the start of year 4 of the project. After reaching the Milestone as planned for this Task, we generated very useful spatial information that is in review at *Applied and Environmental Microbiology* at the time of writing this report.

5.4.1 Task C logic

The intent for this Task was to understand how early modifications made by brown rot fungi facilitate the ingress of enzymes into the cell walls of plants. To do this, we needed some way to track the progress of early stages of brown rot and then visualize the coincident progress of the cellulase enzymes. The original proposal was to purify the endoglucanase from *Postia placenta*, raise antibodies to it (part of Task B due to the need for solid-state extracts), and then use transmission electron microscopy (TEM) to localize the endoglucanase during decay. In April of 2011, we came to the conclusion that this would likely have an issue in terms of synthesis if the endoglucanase

ingress was not apparent. This was based on porosity information showing only modest improvements in porosity (from 12 to 38 Å) relative to the large size of the endoglucanase enzyme (>60 Å). Therefore, we changed tack in this Task to instead focus on a range of size markers as probes for porosity as well as a spatial sampling approach to reconstruct, not image, the colocalization of oxidative and enzymatic reactions during brown rot. This adaptation yielded very satisfying and useful results that did not lose sight of the core question of spatial colocalization.

5.4.2 Size probes for microscopy

The first size markers proposed as an alternative to using a single, large endoglucanase to gauge cell wall porosity during brown rot were 1) triose phosphate isomerase, rabbit muscle (26,600 Da), 2) Myoglobin, horse heart (17,000 Da), 3) alpha-Lactalbumin, bovine milk (14,200 Da), 4) Aprotinin, bovine lung (6,500 Da), 5) Insulin chain B, oxidized, bovine (3,496 Da), 6) Bradykinin (1,060 Da), and 7) Bradykinin Fragments (904.02 Da, 756.85 Da, 572.66 Da), using anti-Bradykinin receptor B1 antibody produced in goat to allow us to use antibodies and gold-labeling to determine ingress relative to size. Then, in Summer 2011, we tested feasibility of using quantum dots (qDots) as more inert probes with potential to 1) avoid antibody steps and the need for secondary probes, and 2) utilize the confocal laser scanning microscope (CLSM) and allow colocalization of reactions with the fungal hyphae imaged within wood cells. This gave satisfying results that also matched those from previous studies of porosity.

5.4.3 Imaging

To produce imaging samples, we inoculated wood substrate with our model fungus *Postia placenta* in order to generate a time series and to verify the probes of choice. We infiltrated decayed material while fresh with qDots in a range down to 2 nm. These qDots have inert qualities, fluorescence for quantification of location in addition to qualifying location using CLSM, and potential for viewing in transmission electron microscopy. We verified our qDots against the background of the wood cell wall, including wood from the decayed time series alongside control, non-decayed wood. A FITC-WGA dye that binds specifically with chitin in the fungal cell walls was also used to colocalize hyphae from *P. placenta* (Figure 3) Here, the goal was to verify the potential to distinguish qDot fluorescence against the autofluorescence of wood cell walls as well as preliminarily assess the resolution potential of our CLSM system at the University of Minnesota.

We compared thin-section material from *P. placenta*-decayed wood with control wood, in this case pine due to ease of liquid penetration and fluorophores (Figure 4). Inoculated wood was infiltrated with a non-crystal forming tissue freezing medium, cooled to -20°C and sectioned to 30 μm with a freezing microtome. Wood sections were to be mounted on treated glass slides to help with adhesion, hydrated with phosphate buffered saline (PBS), pH 7.4 for 10 minutes and dyed with qDots at a single high dilution of 1:200 stock:deionized water, to ensure saturation of pores. The stock was an 8 μM solution in 50 mM borate at a pH of 9.0. Sections were rinsed with PBS solution, a cover slip mounted and were viewed on a Nikon C1 Spectral Imaging Confocal Microscope. Results, as in previous studies, suggested that even these small probes at late stages of decay (8 weeks in pine wafers) could not penetrate the wood cell wall. This supported the change in approach to utilize smaller probes but suggests, as other have before, either that the oxidative pretreatment is the prevalent decay mechanism or that the porosity as decay progresses is not static or slightly increasing. Understanding the dynamic changes in lignin during brown rot, it is possible that porosity may increase and then decrease with de- and re-polymerization of lignin.

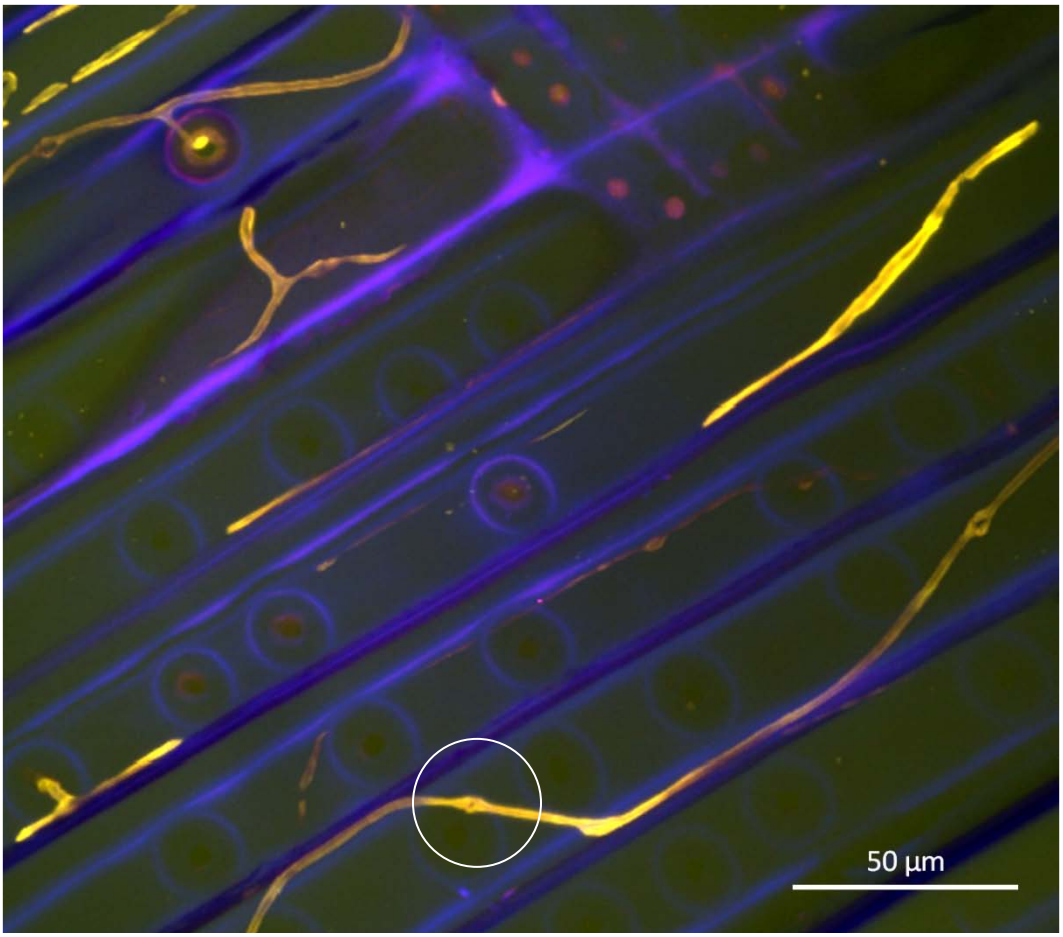

Figure 3 – WGA-FITC fluorophore staining chitin in the cell wall of *Postia placenta* hyphae. Hyphae (yellow) are shown ramifying pine cells (blue with bordered pits), and the circular septa are circled, a unique feature of *P. placenta* as opposed to clamp connections typical of other Basidiomycete fungi. This hyphal stain allowed us to easily colocalize hyphal progress. The inset, below, shows a hypha (visible in the upper image) using the bordered pit for egress cell-to-cell in pine, a growth pattern forced by using cross-sectioned pine as thin 'wafers.'

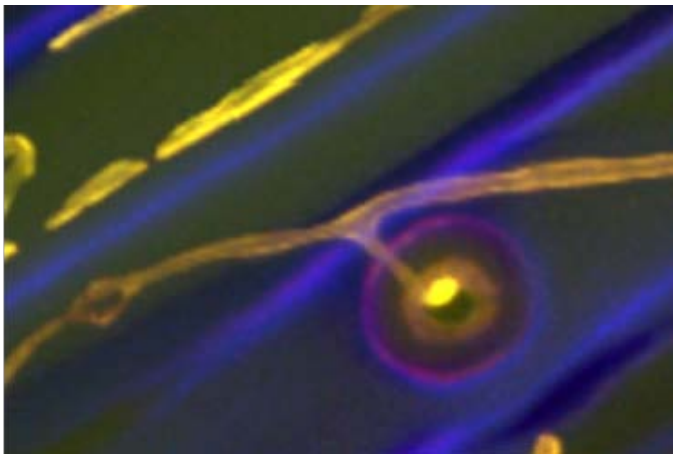

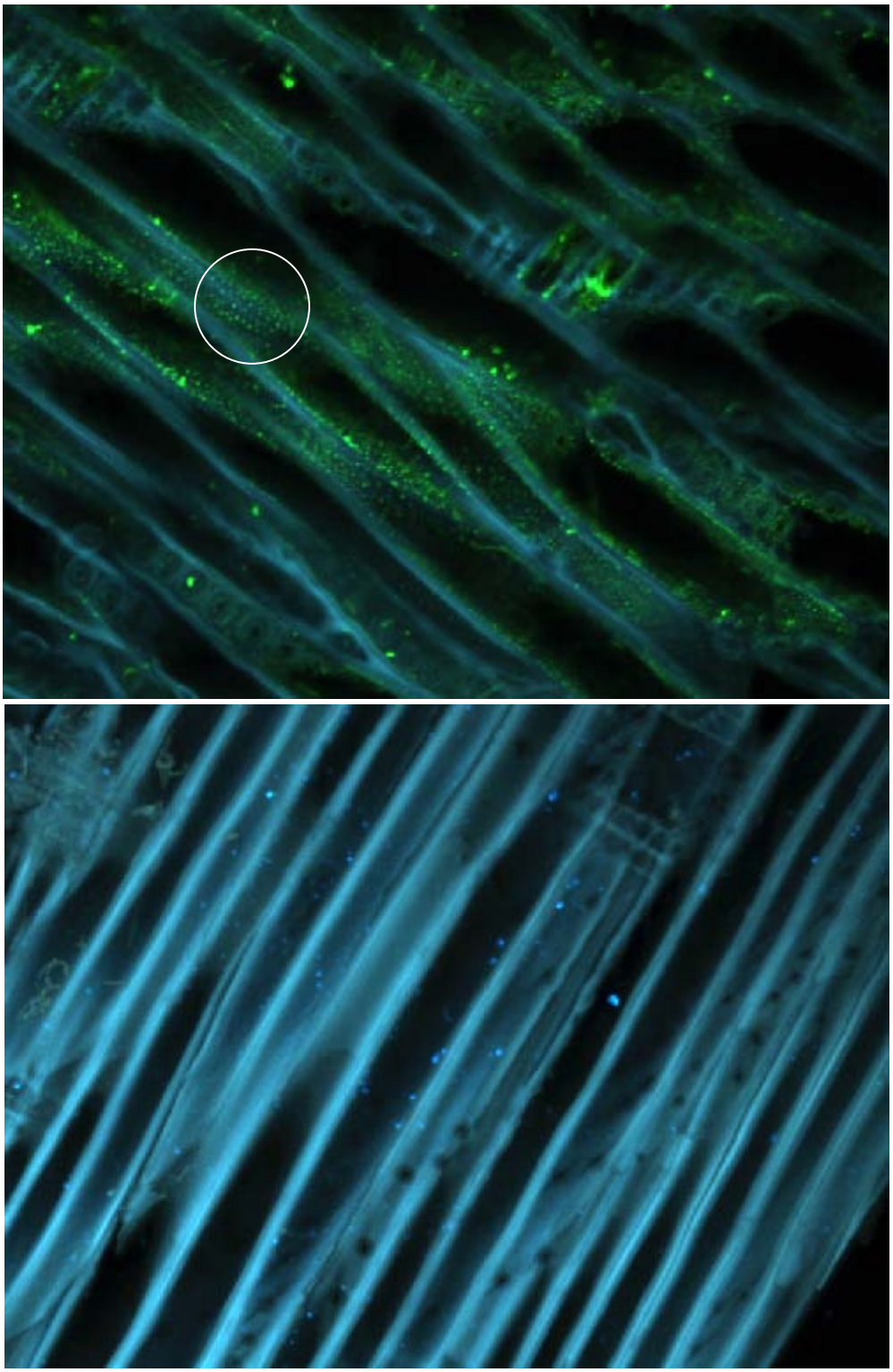

Figure 4 – Non-degraded pine (top) and wood degraded 30 days by *Postia placenta* (bottom), cryo-sectioned to ≈30 µm and infiltrated with quantum dots (qDots are green emission). Field of view is ≈300 µm and images are rendered from stacked optical tomes over a 10 µm range at 50 nm increments. Circle is area of patterned dispersion with some ingress into secondary cell wall, a feature lost at day 30.

5.4.4 'Wafer' trial

A second spatial campaign was initiated during this Task, one that was focused on using physical sampling across a thin-sectioned wafer to mark progress of the fungus, its oxidative reactions, and its enzymes. The approach used here was similar to snapping 60-70 pictures in a row and stitching them together to construct a panorama. Although the porosity images provided some evidence that enzyme ingress was not possible even at late decay stages, this spatial wafer design showed an enzyme front coincident with oxidative tissue modifications suggesting the enzyme is indeed active at early decay stages and its characteristics in the presence of oxidative radicals as well as its general role/contribution to brown rot needs to be resolved. Brown rot cellulases are constitutively produced, unlike white rot fungi, so it would make little sense energetically for endoglucanase to be secreted without access to the cell wall or at least to oligomers for saccharifying.

To create these wafer microcosms, 30 ml of 2% malt extract agar was solidified at the bottom of pint mason jars and inoculated from an active hyphal front with a 1 cm^2 plug of fungal inoculum from *Postia placenta* (isolate MAD 698-R). A sterile circular black autoclaveable plastic mesh (co-polymer Gutter Guard, Amerimax, PA, USA) cut to fit the jars was then laid flat on the surface. When the mycelium was well-developed (2-4 weeks), spruce, a low permeability wood species, was added as wafers propped vertically against the sides of the jars. For wood 'wafers,' kiln-dried spruce was cut into 7 mm thick wafers with the largest plane being the transverse section (23 x 70 mm). This design was adopted to force hyphae growing up the wafer to travel in the transverse plane and across the grain but not across annual rings (tangential axis), in order to minimize variability and maximize cell-to-cell gradients for spatial analyses.

Wood was sectioned into small portions and analyzed individually prior to re-assembling as a composite (Figure 5). When harvested, the distance of visible fungal growth up the wafers was recorded, hyphae were scraped from the surfaces, and the wafers were stored at -80°C. For the first experiment wafer harvests, two adjacent 3 mm strips (strips=vertical cuts) were carefully cut from the fresh wafer over the 70-mm length from the bottom to the top using a razor and a vice as a straight edge, and without thawing the wafers (Figure 5). One of these strips was intended for endoglucanase (EG) analysis and one for microscopy. For the EG activity analysis, the strip (3 x 7 x 70 mm) was sectioned again into seventy 1-mm sections (sections=horizontal cuts) along the entire 70 mm length, and each of these sections was cut into three strips, each 1 x 1 x 2.5 mm. The remaining 17 x 7 x 70 mm strip was stored at -80°C until sectioning for modification analyses.

For a second experimental decay series, the goal was to reduce analyses per wafer section to reduce variability and improve resolution of reaction fronts, particularly for EG. Wafers (60 mm) were bisected from bottom to top to create two strips (11.5 x 7.5 x 60 mm), one to measure DAS and the other EG activity (Figure 1). The EG strips were frozen and stored at -80°C until processing. The EG strips were thawed to room temperature and sectioned into sixty 1-mm sections and air dried overnight. Enzyme analyses for each diced section were performed as in round one. For dilute alkali solubility (DAS) analysis, strips were oven-dried and stored at -20°C prior to processing. The strip was cut into thirty 2-mm sections giving enough sample weight to be gravimetrically measured for DAS (%) as in experiment one.

For analysis of cellulase activity, a single strip cut from the fresh wafer was added per well to a 96-well microtiter plate for EG extraction and analyzed using a $1/10^{th}$ scale Azo-carboxymethylcellulose (CMC) EG assay method as per manufacturer instructions (Megazyme,

Bray, Ireland). Wood strips added to wells in 96-well plates were sealed and incubated at 40°C and at 120 rpm in 50 µl sodium acetate buffer (100mM, pH 4.6) for 3 h. Azo-CMC was then added and the plate returned to 40°C for 30 min. The reaction was stopped and the samples vortexed, centrifuged, and supernatant absorbance analyzed at 590 nm following the Azo-CMC manufacturer guidelines. Activity was expressed as CMC units (CMCU) without correcting for protein concentration in order to focus on overall activity and not per-enzyme potential.

Hyphal distance vertically up the wafers was recorded for each sampled wafer and generally was uniform as a horizontal front moving up the wafer. The visible hyphal front was matched by analysis of hyphal progress within wood cells by fluorescent staining of chitin and CLSM. Wood pH, solubility in dilute alkali solution, and lignin demethylation were measured from the 17-mm strip and from sections ground to 40 mesh. The pH and DAS could be measured easily from single sections and were measured following detailed protocols. Lignin modifications were analyzed using ^{13}C TMAH as before. In our Schilling et al. (2012) paper, the most sensitive lignin modification to brown rot was the increase in G4 demethylation residues, possibly attributed to oxidative alteration of the alpha carbon on lignin's propanoid chain to yield vanillic acid during TMAH thermochemolysis. Samples were pooled for TMAH relative to their distance from the EG front, determined first. Using the EG front as our guide, we overlay hyphal fronts for individual wafers and pH and DAS measures as matched data per wafer. The pooled TMAH data was used to infer the extent of oxidative lignin modification at the wafer base and up to 6 mm ahead of the EG front, as a mean value to be colocalized using the EG front as a baseline among wafers.

Results from this work, an effort that more recently leveraged contributing funding from a DOE BER program grant and a University of Minnesota Initiative for Renewable Energy and the Environment (IREE) grant, showed coincident EG and oxidative fronts, with the exception that dilute alkali solubility increased slightly ahead of the EG front. This DAS is a measure of depolymerization of carbohydrates, so it suggests along with the TMAH data that there is not a large (if any) partitioning of reactions but that the endoglucanase is also present along with oxidative reactions. This would explain the porosity findings, given there is no increase over time during decay. Endoglucanase is present, whether permeating the cell wall or not.

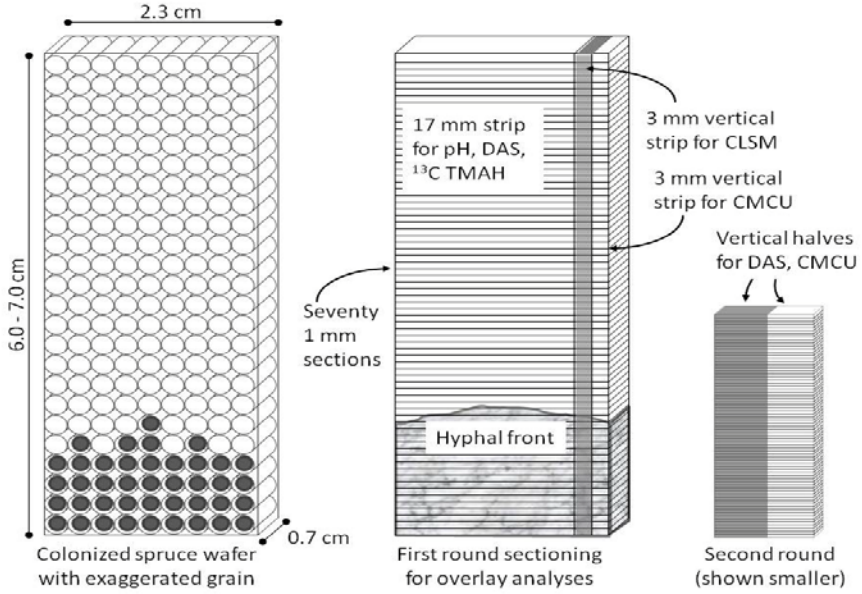

Figure 5 – Wafer orientation, showing fungal colonization point and sampling regime.

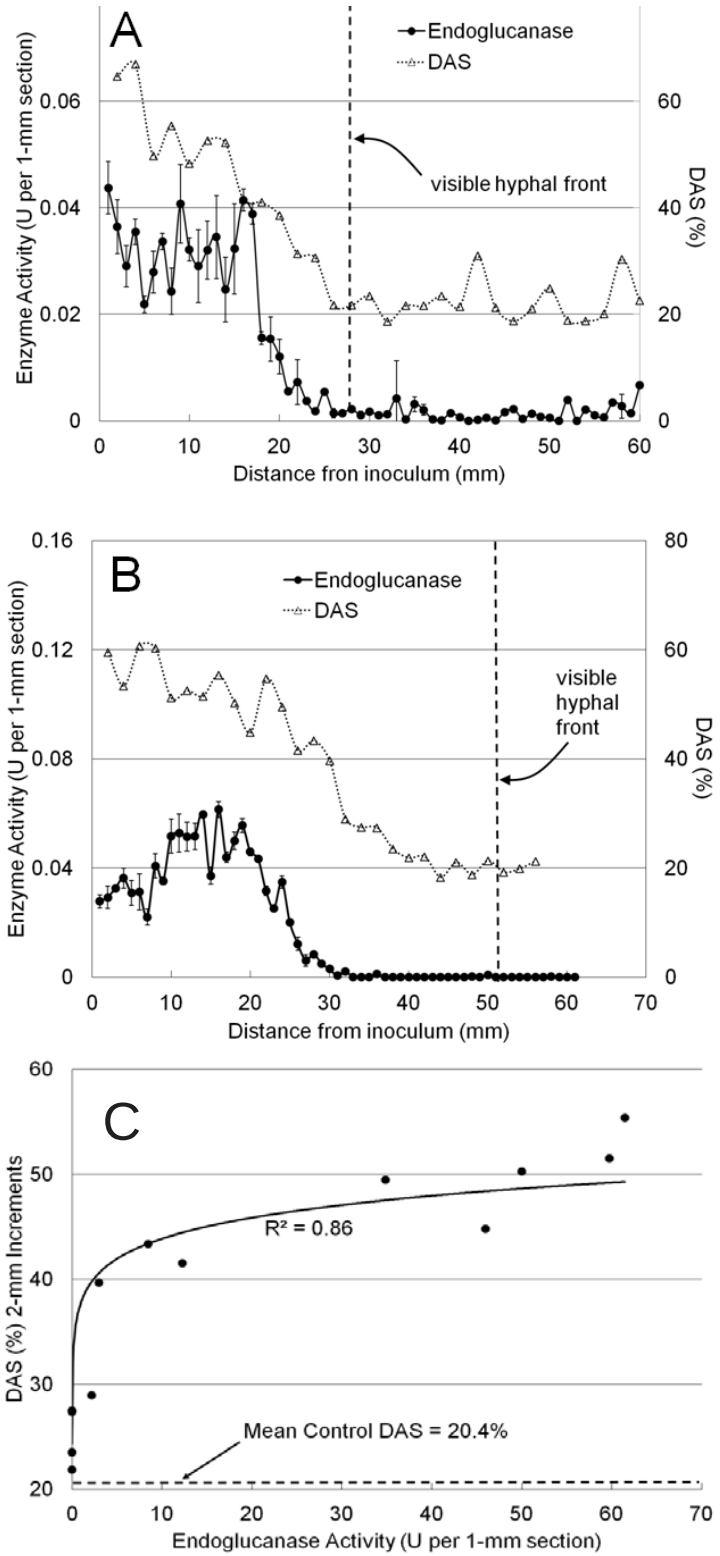

Figure 6 – Endoglucanase activity as a function of distance up spruce wafers, the largest face in the transverse plane. (A) shows the trend at 2 wks colonization, (B) at 18 d, and (C) the correlation between cellulase and dilute alkali solubility, a measure of early depolymerization. This relationship indicates a 'stagger' between oxidative and enzymatic reactions during early brown rot, but behind the advancing fungus.

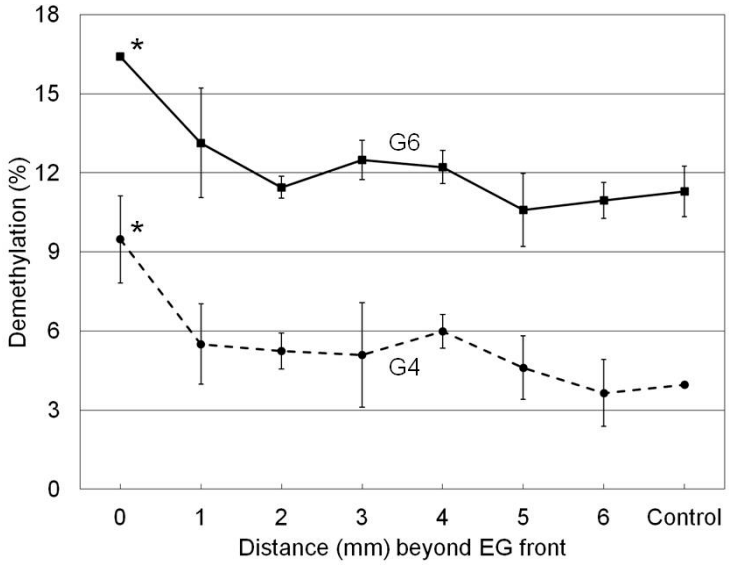

Figure 7 – Lignin demethylation (as measured using TMAH thermochemolysis) as a function of distance ahead of the endoglucanase (EG) front proceeding up a spruce wafer colonized by *P. placenta*. Note that in Figure 6, the hyphal front is well beyond the EG front, indicating that the oxidative reactions are coincident with EG presence but behind of progressing fungus.

5.4.5. Conclusion from Task C

Spatially, the current brown rot paradigm gives no alternative to the separation/partitioning of early brown rot oxidative reactions (Fenton-based) from enzymatic hydrolysis of carbohydrates. This is theorized possible because of gradients in pH, porosity, and perhaps lignin adsorptivity. Unfortunately, however, previous research from the early 1990s suggests that even at late stages of brown rot decay, wood cells remain impervious to cellulases, which are too big to penetrate the largest of pores produced by the oxidative pretreatment. Our results confirm an issue with porosity, but also show high endoglucanase activity concurrent with two different oxidative tissue modifications made to wood cells. This suggests that the constitutive production of cellulases is important, but that we have not fully characterized their role. We would say we have, even, underestimated their role. Early stages of brown rot are devastating to strength in wood. This has precipitated a great deal of research into one (the oxidative), not both steps required for the fungus to eat wood. It is likely that the enzymatic system involved in metabolism of carbohydrates is more efficient than given credit and that approaching this issue from a systems perspective is imperative.

5.5. Task D

The final Task was to apply the knowledge learned from the other Tasks toward applying a mimic of the brown rot pretreatment. Because the first Tasks suggested no particular synergy between early brown rot pretreatments of the plant cell walls, we were able to approach this Task using commercial cellulases instead of extracted crude filtrates. The goal was to apply the theory of brown rot, where Fenton chemistry (reduced iron and hydrogen peroxide form hydroxyl radicals) drives tissue depolymerization and lignin demethylation, while cellulases remove the cleaved oligomeric carbohydrates and release fermentable monomers. Because the mimic could reveal

insight into the potential in the fundamental physiological system, we started this Task ahead of schedule and the Deliverables were achieved on time. The Milestone was also achieved early, and we kept the Task open in order to test potential options for the mimic until project completion.

5.5.1 Task D logic

Brown rot fungi are theorized to use low molecular weight agents, not enzymes, to initiate a pretreatment of biodegradation. This pretreatment relies on production of hydroxyl radicals away from the fungal hyphae in wood cell walls. More importantly for bioconversion, absence of enzymes in the pretreatment step gives potential to mimic the approach chemically or consolidate aspects into a chemical pretreatment approach. Our goal was to extend the knowledge from our work and past research to better mimic this pretreatment for application. Past research has been very sparse in terms of chemical mimics. We wanted to go beyond simply adding the Fenton reagent of reduced iron and hydrogen peroxide (reaction below), and instead add aspects of control for this reaction that might better control the spatial production of radicals as well as give a better chance for a mimic given the lack of fungal presence. This included a manganese-based mimic that showed some promise in older work aimed at chemical depolymerization of cellulose.

Fenton reaction: $Fe^{2+} + H_2O_2 \rightarrow$ -OH + Fe^{3+} + HO· (mediated by iron-reducing chelator)

5.5.2. The Fenton mimic

The Fenton mimic as a pretreatment prior to saccharification has been tried in the past on at least one occasion in another laboratory in Europe, and the Fenton reagents have been used to treat wood and compare modifications to those in early brown rot. Beyond similarities and modest increases in yield after pretreatment, no researchers of whom we know have ever gone beyond the additions of reduced iron and hydrogen peroxide. We therefore included the simple Fenton mimic but then progressed complexity toward a mimic that truly reflected how brown rot proceeds. In this Fenton mimic effort, we included the reducing 'chelator' theorized to be involved in generating reduced iron within the wood cell walls (dimethoxyhydroquinone, DMHQ), as well as a reducing agent to recycle the chelator once oxidized while reducing iron. We also bound iron on cellulose to attempt to direct production of hydroxyl radicals near the substrate target, and we used oxalate as a variable that has been often theorized to improve iron mobility without sacrificing its availability to be reduced. All reactions were in a controlled and relevant pH, and 'success' was measured as saccharification yields relative to controls.

To do this, we pretreated aspen wood flour with the components of the brown rot extracellular suite, including a chelator mixture that not only takes advantage of the hydroquinone 2,5-DMHQ, synthesized from dimethoxybenzoquinone (DMBQ) but also includes several other chelators and redox reagents that our models predicted would improve yield. The specifications on the conditions are listed below as three treatments (the mediated Fenton mimic, an oxalate treatment, and a control.

For the chelator-mediated Fenton reaction (CMFR) treatment, 0.5 g of Aspen flour (40 mesh) with 2.06% moisture was mixed with 200 mL of 10mM oxalate buffer (pH = 4.2) at room temperature in a 250 mL Erlenmeyer flask. 0.795 mg (20 μM) of $FeCl_2 \cdot 4H_2O$ were added after 10 minutes of stirring. 0.681 mg of DMHQ (20 μM) and 4.421 mg (650 μM) of H_2O_2 were added

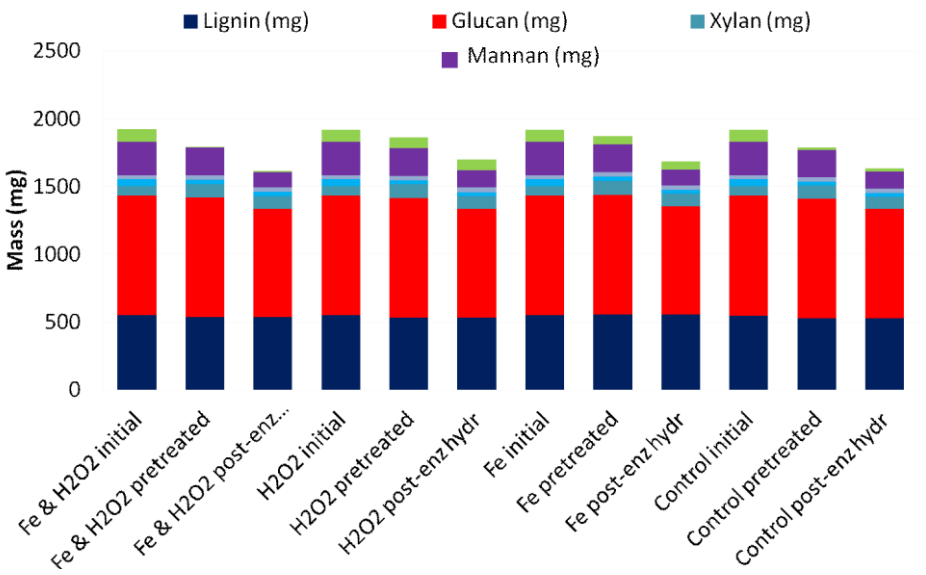

Figure 8 – The simple mimic, and yields (per original) of sugars and lignin after pretreatments with simple Fenton reagent combinations.Green are 'extractives' (EtOH extracts). The 'post-enz' columns are those of determined sugars after saccharification with cellulases. These results demonstrated the low success rate when not incorporating a chelator to reduce iron in closer proximity to tissue.

after an additional 30 minutes of stirring. After 20 hours, 174.1 mg (1 mM) of $Na_2S_2O_4$ was added to the mixture, which was allowed to stir for 9 more hrs before removal and subsequent washing (5 X 45 mL distilled H_2O) of the aspen flour via centrifuge.

Because oxalate has been theorized to be the sole iron-reducing agent as well as hydrolytic driver of brown rot (both unlikely), we included an oxalate treatment separately. For this oxalate treatment, 0.5 g of Aspen flour (40 mesh) with 2.06% moisture was mixed with 200 mL of 10mM oxalate 'buffer' (pH = 4.2) at room temperature in a 250 mL Erlenmeyer flask. The aspen flour was added after 29 hours, 174.1 mg (1 mM) of $Na_2S_2O_4$ was added to the mixture, which was allowed to stir for 9 more hrs before removal and subsequent washing (5 X 45 mL distilled H_2O) of the aspen flour via centrifuge.

The control treatment for this trial was to mix 0.5 g of Aspen flour (40 mesh) with 200 mL of distilled water at room temperature in a 250 mL Erlenmeyer flask. The aspen flour was added after 29 hours, 174.1 mg (1 mM) of $Na_2S_2O_4$ was added to the mixture, which was allowed to stir for 9 more hrs before removal and subsequent washing (5 X 45 mL distilled H_2O) of the aspen flour via centrifuge.

The washed aspen flour from each pre-treatment was placed in an aluminum pan to air-dry before the moisture content of a portion of the material was measured. Using this moisture content for the total pre-treated mass, it was found that the weight loss for the CMFR, control, and oxalate samples were 1.80%, 4.72%, and 5.36% respectively. Sugar analysis via HPLC of the pre-treatment reaction supernatant exhibited no monosaccharide in any pre-treated material, prior to saccharification. Prior to saccharification, treated powders were characterized to track lignin and

carbohydrate loss, as well as define the cellulose content in fresh or air dried samples to normalize enzyme loadings. Saccharification was done as usual at 50°C with rotation, using full strength Celluclast 1.5L and Novozyme 188, added at a set ratio relative to the cellulose content in the samples. This approach is relatively high throughput, allowing us to work in smaller scintillation volumes but without sacrificing by increasing the variability, an increasing issue when treating increasing smaller volumes of wood powder which may vary in particle size as well as wood origin (sapwood vs. heartwood, etc.).

Interestingly, one of these additions, oxalate, did not enhance mobilization or transfer of iron as hypothesized to improve Fenton occurrence or pretreatment efficacy, but in the chelator mix, provided a nearly two-fold enhancement in preatreatment, verified by subsequent saccharification of the powder (Figure 9). This was promising, fairly early in this research timeline, and we pursued this further keeping in mind substrates that resemble real-world options, like wood chips not powder, and continuing to use the model to guide our variable selections. One barrier, as discussed with our transition team collaborator at ADM, is that without consolidation with a downstream step, the Fenton mimick must at this point four years later compete with a well-developed dilute acid pretreatment approach. Therefore, our discussions concerning the transition of these Task results involves both a techno-economic analysis of both biological and chemical pretreatment options, as well as probing the brown rot mechanisms of consolidation in nature. The fact remains that brown rot fungi, if using the mechanism as theorized, consolidate two incompatible reactions, one oxidative and the other enzymatic, and this is an unrealized goal in bioconversion of biomass.

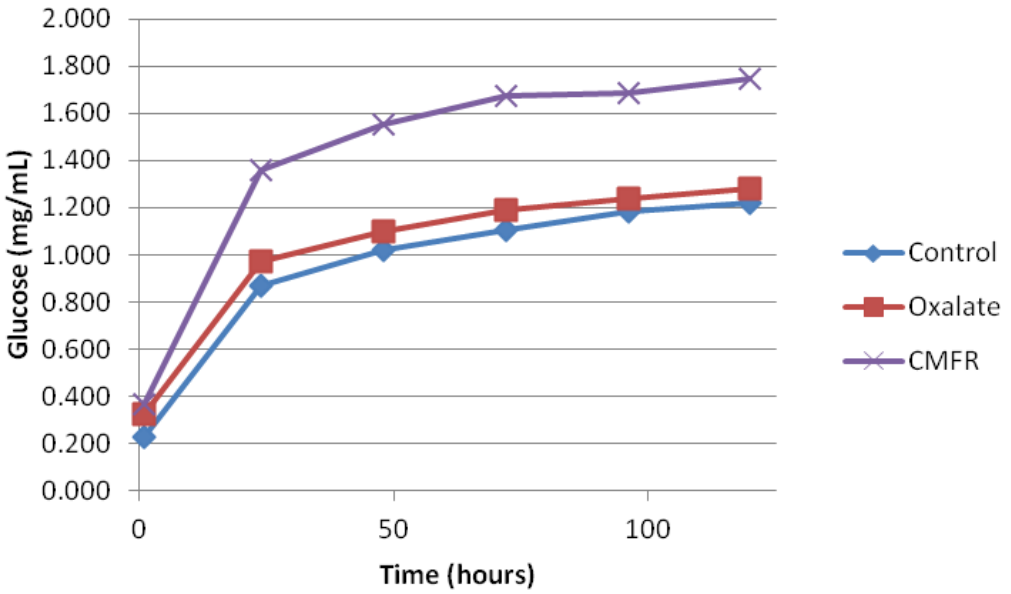

Figure 9 – Glucose release over the course of saccharification from aspen wood powder (40 mesh) treated with a chelator mixture, simulating the brown rot low molecular weight chelator system known as "Gt chelator" in the literature and referred to in the graph as CMFR, for chelator-mediated Fenton reaction. Oxalate alone gave little enhancement over the control.

5.5.4. Transition objectives

Our cost-share partner, ADM, has been very active meeting and discussing the project as it progressed. There have been two key areas where our contact, Dr. Charles Abbas, has been particularly insightful; 1) the biological pretreatment success, which was greater than expected, and 2) the mimic approaches and results. For the biological pretreatment, Charles has helped with back-of-the-envelope calculations for costs when yield loss is compensated by cost gain, as well as the importance of incorporating waste and transportation costs. Above all, these discussions led us to include an extra, more resolved decay time series and use correlations in our synthesis for the 2012 *Bioresource Technology* paper to allow prediction of yield. This was not something we were planning, and it increased the audience for that paper significantly by broadening the impact through synthesis of a complex data set. Concerning the mimick, Charles has also been helpful with understanding costs but also scale-up, which is a critical stumbling point for many studies and for our work will need to incorporate real-world feedstock issues. These contributions are included here as a 'transition' section because the conversation is ongoing, and we have harnessed the collaboration to secure funding focused on the more basic aspects of the spatial analyses in Task C. This allows us to move our project forward, beyond the funding cycle of this award.

5.5.5. Conclusions from Task D

Task D provides the framework for a functional mimic and a data set that is still being processed for publication. Part of the data set will also require conversion of reducing sugar data and raw yields to true yields per original contents. Unlike the rigid treatment structures of the biological work, here we were free to assess a very large number of pretreatment options and mixtures. Our conclusion is that a mimic works but that the kinetics are difficult to control. We believe this is due to spatial control, not temporal, and that localization of reactions in close contact with the carbohydrates is indeed useful but perhaps better explored with manganese. The transition objectives with ADM have also been ongoing, and it is clear we have made wise collaboration here. With funding in place for the basic spatial reaction partitioning objectives, the road forward based on these findings and discussions is to flesh out the details of spatial reaction control and then build back into our applied objectives the knowledge gained from those efforts.

6. Project Output

6.1. Technical Publications

Schilling, J.S., Blanchette, R.A., Duncan, S.M., Filley, T.R., Jurgens, J.A, and Presley, G.N. (in review) Colocalization of oxidative and enzymatic reactions during fungal brown rot of wood. Applied and Environmental Microbiology. (AEM03561-12).

Schilling, J.S., Ai, J., Blanchette, R.A., Duncan, S.M., Filley, T.R., and Tschirner, U.W. (2012) Lignocellulose modifications by brown rot fungi and their effects, as pretreatments, on cellulolysis. Bioresource Technology 116:147-154.

Duncan, S.M. and Schilling, J.S. (2010) Carbohydrate-hydrolyzing enzyme ratios during fungal degradation of woody and non-woody lignocellulosic substrates. Enzyme & Microbial Technology 47:363-371.

Tewalt, J. and Schilling, J.S. (2010) Assessment of saccharification efficacy in the cellulase system of the brown rot fungus *Gloeophyllum trabeum*. Applied Microbiology and Biotechnology. 86:1785-1793.

Schilling, J.S., Tewalt, J., and Duncan, S.M. (2009) Synergy between pretreatment lignocellulose modifications and saccharification efficiency in two brown rot fungal systems. Applied Microbiology and Biotechnology 84: 465-475.

6.2. Presentations & Posters

Schilling, J.S., Ai, J., Blanchette, R.A., Duncan, S.M., Filley, T.R., Jurgens, J., Kaffenberger, J., Presley, G.N., Tschirner, U.W. Reaction partitioning by wood-degrading fungi - doing the two step without tripping. Mycological Society of America (MSA) annual meeting, New Haven, CT, July 17, 2012.

Schilling, J.S. Wood-degrading fungi: Application, implication and oversimplification. *For* Department of Plant Pathology, University of Minnesota, March 5, 2012.

Duncan, S. M., Schilling, J. S. Measuring fungal cellulolytic enzyme activity in degrading wood. International Research Group-Wood Protection-IRG/WP. Queenstown, New Zealand May 9, 2011.

Schilling, J.S. Decay fungi for biofuels: How a rot got hot. *For* Institute on the Environment (IonE) Frontiers in the Environment Series, University of Minnesota, April 20, 2011.

Schilling, J.S. Lignin as a facilitator, not a barrier, during saccharification by brown rot fungi. DOE Biochemical Platform Review, Denver, CO, February 13, 2011.

Duncan, S.M. and Schilling, J.S. Cellulolytic enzyme ratios during fungal degradation of lignocellulose. For Forest Products Society (FPS) annual meeting, Madison, WI, June 21, 2010.

Duncan, S.M. and Schilling, J.S. Cellulolytic enzyme ratios during fungal degradation of lignocellulose. For Forest Products Society (FPS) annual meeting, Madison, WI, June 21, 2010.

Tewalt, J. Assessment of saccharification efficacy in the cellulase system of the brown rot fungus *Gloeophyllum trabeum*. Master of Science Thesis – University of Minnesota – Natural Resource Science and Management (NRSM). August 28, 2009.

Schilling, J.S. Lignin as a facilitator, not a barrier, during saccharification by brown rot fungi. DOE Biochemical Platform Review, Denver, CO, April 16, 2009.

Tewalt, J.P., Duncan, S.M., and Schilling, J.S. Wood modifications by brown rot fungi may offer competitive advantage for their own cellulases. American Phytopathological Society (APS) Centennial Meeting, Minneapolis, MN, USA, July 30, 2008.

Schilling, J.S., Tewalt, J., Duncan, S.M. Saccharification by brown rot fungi: a model approach. Forest Products Society (FPS) – Society for Wood Science and Technology (SWST) Joint Annual Meeting, Boise, ID, June 22, 2009. (poster)

Schilling, J.S., Tewalt, J., and Duncan, S.M. Saccarification by brown rot fungi. E3 Conference, St. Paul, MN, November 18, 2008. (poster)

Tewalt, J.P. Schilling, J.S., and Duncan, S.M. Brown rot as a model system for improved bioprocessing. Biobased Industry Outlook Conference. Ames, IA, September 9, 2008. (poster)

Tewalt, J., and Schilling, J.S. Brown rot bioprocessing: coupling pretreatment and saccharification in wood. Forest Products Society (FPS) International Convention, Saint Louis, MO, USA, June 24, 2008. (poster)

6.3. Emerging Collaborations & Technology Gains

Beyond those developed by this grant, emerging networks/collaborations were established with the following:

Dr. Kenneth Hammel – U.S. Forest Products Laboratory, University of Wisconsin – Spatial localization of brown rot fungal endoglucanases using electron microscopy.

Dr. Ping Wang – University of Minnesota, Biotechnology Institute – Kinetics of a brown rot mimic, using chemicals and a low-molecular weight iron reducing agent.

Dr. Matt Olsen – Texas Tech University – Plant genomics and feedstock amenability to bioconversion.

The technological proficiency gains have been extensive on this project. On the bioconversion aspects, as required to better understand how brown rot fungal mechanisms could be harnessed for an industrially-relevant process, we had to learn or optimize the latter. This includes many standard National Renewable Energy Laboratory (NREL) standard protocols, as well as saccharification to compare natural enzyme systems with those commercialized. This is significant, given the issues with mass loss during decay and the lack of a cellobiohydrolase (CBH) enzyme in the brown rot cellulase system. These approaches, along with the yield calculations that support their results, are published in detail in the publications shared during this grant award period. They are also highly valuable when comparing a mimic approach to a commercially-relevant positive control such as dilute acid pretreatment, which we have also optimized. In addition to this physiochemical know-how, the imaging effort has provided us with a strong set of spatial tools. Cryo-sectioning and image analyses can be difficult with wood samples, particularly when decayed. This know-how remains in-house and is valuable on the fundamental spatial effort going forward.